R-Matrix Scattering Calculations for Iron-Peak Species: Photoionisation of Fe I and Electron-Impact Excitation of Fe II

Ryan T. Smyth *, Catherine A. Ramsbottom and Connor P. Ballance

School of Mathematics and Physics, Queen's University Belfast, Belfast BT7 1NN, UK;
c.ramsbottom@qub.ac.uk (C.A.R.); c.ballance@qub.ac.uk (C.P.B.)
* Correspondence: rsmyth41@qub.ac.uk

check for
updates

Abstract: An abundance of absorption and emission lines of iron-peak species such as Fe I and Fe II can be seen in the spectra of many astrophysical objects. Thus, the accurate modelling of such spectra requires sets of high quality atomic data for these species. In this paper, we present preliminary results from the present electron-impact excitation calculations for Fe II and fine-structure resolved photoionisation calculations for Fe I employing the Dirac atomic R-matrix and Breit–Pauli R-matrix methods. For the Fe II excitation, we compare results with all existing calculations, and for the Fe I photoionisation, we present a sample of level-resolved cross-sections. The calculations and results described throughout will be of use to those requiring high quality atomic data for modelling a wide variety of astrophysical objects.

Keywords: atomic data; electron-impact excitation; photoionisation

1. Introduction

Atomic data for iron-peak species is undoubtedly of great importance for modelling applications in many areas of astrophysics and astronomy. Observations of a wide variety of objects show emission and absorption lines of singly-ionised iron in their spectra, with lines of Fe II dominating the spectra of the symbiotic star AG Pegasi [1] for example. In particular, the work of [2] has shown that transitions between the lowest lying fine-structure levels of Fe II are amongst the strongest and are prominent in the spectrum of P Cygni's nebula. However, the available atomic data for such transitions, obtained from calculations of varying size and complexity, show large discrepancies owing to the difficulty of modelling their open 3d-shell atomic structures. These existing calculations have ranged from small 2–3 term calculations, employing the close-coupling [3] and distorted wave [4] methods, to R-matrix calculations retaining between four and 113 LS terms [5–9] (or 16–142 fine-structure levels for calculations incorporating relativistic effects [6,10–14]) in the target description, to larger more sophisticated R-matrix calculations of [15,16] including 262 levels in the target description. Currently, there exists little to no agreement amongst these calculations with regards to the effective collision strengths for the forbidden transitions, often exhibiting discrepancies of up to factors of three. The present work aims to address this discrepancy and demonstrate the convergence of the effective collision strengths for the important low lying forbidden transitions and extend upon existing models by carrying out a large 716-level R-matrix Breit–Pauli scattering calculation. Furthermore, details of an additional 262-level calculation using the Dirac Atomic R-matrix Codes (DARC) [17] will be presented, corroborating results from the current 716-level Breit–Pauli calculation.

Neutral iron is another important iron-peak species for which accurate atomic data are of crucial importance, the photoionisation of which is a large contributor to the opacities of many astrophysical

objects. All existing photoionisation calculations up to now have been carried out in LS coupling employing a variety of different methods including the central field method [18,19], many-body perturbation theory [20,21] and the R-matrix method [22–28]. However, investigations of [29,30] have demonstrated that fine-structure resolved calculations may reveal additional resonance features that are missed in LS-coupled calculations, potentially affecting any astrophysical modelling that uses these datasets. In this work, we present preliminary results for the fine-structure resolved photoionisation of neutral iron using the Dirac R-matrix method. In the next section, we present our current target models and results of the R-matrix scattering calculations for the electron-impact excitation of Fe II and photoionisation of Fe I.

2. Results and Discussion

2.1. Target Models

The target model for the current Breit–Pauli R-matrix calculation has been based on a six configuration CIV3 [31] calculation 'A1', as discussed in detail in the work of [8], while the current DARC target model, employed in both the excitation and photoionisation calculations, was determined from a large multi-configurational Dirac–Fock calculation (employed with $GRASP^0$ [32,33]) with 20 configurations. A sample of energies from these target models is given in Table 1 and compared to the experimental values in the NIST database [34]. Overall, our target descriptions for both the Breit–Pauli and DARC calculations showed average differences of 10.3% and 9.3%, respectively, with experimental values provided in the NIST database. We note that the present 20 configuration, DARC target model has been incorporated into both the electron-impact excitation calculations for Fe II and the photoionisation calculations for Fe I.

Table 1. Sample of fine structure energies (in Rydbergs) of the first 15 levels of Fe II from the present Breit–Pauli and DARC calculations compared to experimental energies given in the NIST database.

Term	J	NIST	Breit–Pauli	DARC
$3d^6 4s\ ^6D$	9/2	0.00000	0.00000	0.00000
$3d^6 4s\ ^6D$	7/2	0.00351	0.00398	0.00323
$3d^6 4s\ ^6D$	5/2	0.00608	0.00695	0.00562
$3d^6 4s\ ^6D$	3/2	0.00786	0.00903	0.00728
$3d^6 4s\ ^6D$	1/2	0.00890	0.01025	0.00825
$3d^7\ ^4F$	9/2	0.01706	0.02786	0.01757
$3d^7\ ^4F$	7/2	0.02215	0.03315	0.02197
$3d^7\ ^4F$	5/2	0.02586	0.03707	0.02523
$3d^7\ ^4F$	3/2	0.02841	0.03977	0.02748
$3d^6 4s\ ^4D$	7/2	0.07249	0.07232	0.10600
$3d^6 4s\ ^4D$	5/2	0.07647	0.07694	0.10983
$3d^6 4s\ ^4D$	3/2	0.07910	0.08005	0.11222
$3d^6 4s\ ^4D$	1/2	0.08062	0.08186	0.11363
$3d^7\ ^4P$	5/2	0.12279	0.14864	0.10860
$3d^7\ ^4P$	3/2	0.12460	0.15096	0.11062

2.2. Fe II Electron-Impact Excitation

In Figure 1, we present preliminary results, in the form of effective collision strengths, for the $3d^6 4s\ ^6D_{7/2}$ - $3d^6 4s\ ^6D_{5/2}$ forbidden transition and compare with available existing results in the literature. It is evident that there was very good agreement in terms of shape and magnitude between the current 716-level Breit–Pauli and 262-level DARC calculations, and also with the existing effective collision strengths of [15]. We further note that good agreement was seen with the reported results of [11] at an electron temperature of 10^4 K; however, the remaining results at lower temperatures were slightly larger than the current results. Comparisons with additional effective collision strengths of [10] (and those of [14] obtained from an extension of the work of [10] to lower temperatures) all

fell much too low due to the omission of odd parity states in the target description. It is evident from these comparisons that, for the first time, near-convergence of the effective collision strengths had been reached for this low-lying forbidden transition across a large temperature range, which will be of interest for future modelling of a wide variety of astrophysical objects.
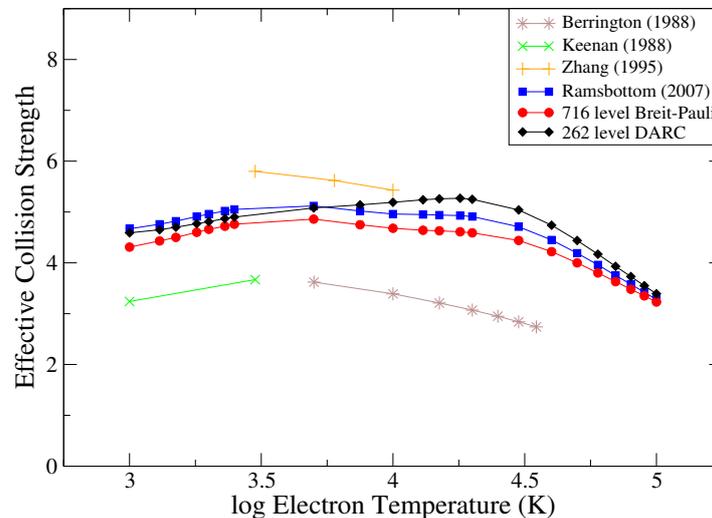

Figure 1. Effective collision strengths for the $3d^6 4s\ ^6D_{7/2}$ - $3d^6 4s\ ^6D_{5/2}$ forbidden transition. Red circles and black diamonds are the current Breit–Pauli and DARC results, respectively. Blue squares are the results of [15]; orange pluses are the results of [11]; green crosses are the results of [35]; and brown stars are the results of [10]

2.3. Fe I Photoionisation

Now, we present a sample of preliminary results from the current fine-structure resolved Fe I photoionisation calculations. We will focus only on levels in the ground term complex to illustrate our results. We first note that this 262-level DARC calculation yielded an ionisation potential of 0.734 Ryd compared to the experimental value of 0.581 Ryd, giving an error of 26.3%. However, despite this discrepancy, the energy level separations amongst the levels in the ground term were in good agreement with the experimental values. As an example, the calculated energy of the Fe I $3d^6 4s^2$ $^5D_1$ level in the ground term was 0.0079 Ryd above the $3d^6 4s^2\ ^5D_4$ ground level, and compared with the experimental value of 0.0081 Ryd, gave a small error of 2.5%. The associated photoionisation cross-section for this $3d^6 4s^2\ ^5D_1$ level is presented in Figure 2.

We note that in our calculation, the N+1 correlation functions associated with all 20 N-electron target configurations were determined. However, the truncation of our large Fe II target structure at 262 levels ultimately resulted in an over-correlated description of the N+1 electron (Fe I) system, leading to an inflated value of the Fe I ionisation potential. To account for this over-correlation, we may remove configurations of the N+1 electron system that are associated with highly excited states of the Fe II target that were not included in the calculation, while simultaneously leaving the Fe II target structure unchanged. As a result, removing these N+1 configurations would lead to an improvement of the Fe I ionisation potential due to a reduction in the excess correlation effects.

Given the above considerations, to correct for the discrepancy in the Fe I ionisation potential, we have carried out sample calculations in which we removed all N+1 configurations associated with the $3p^5 3d^7 4s$, $3p^5 3d^7 4p$ and $3p^5 3d^7 5s$ Fe II target states. This led to a slight correction of 0.010 Ryd to the ionisation potential. Going further and removing the N+1 configurations associated with the $3p^4 3d^9$, $3p^5 3d^6 4s 5s$ and $3p^4 3d^7 4s^2$ Fe II target states resulted in an overall correction of 0.028 Ryd. In Figure 2, we provide an additional cross-section from a reduced calculation for the Fe I $3d^6 4s^2\ ^5D_1$ level. As is evident from this additional calculation, we see that removing these N+1 configurations results in a

shift of the photoionisation cross-section to the left, with negligible changes to the resonance structures, magnitude and shape of the cross-section, suggesting that we may simply shift all cross-sections by a fixed amount to correct for the ionisation potential.
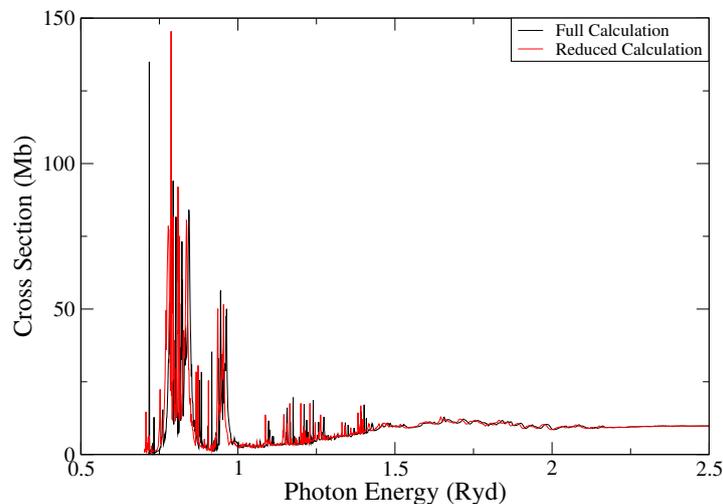

Figure 2. Photoionisation cross-section of the Fe I $3d^6 4s^2\ ^5D_1$ level in the ground term. The black line is the result from the full calculation with N+1 configurations included, and the red line is the result of a reduced calculation with N+1 configurations removed.

3. Conclusions

In this work, we have presented a selection of results from large-scale R-matrix calculations for the electron-impact excitation of singly-ionised iron and for the photoionisation of neutral iron. Discrepancies amongst existing effective collision strengths for the electron-impact excitation of Fe II have been addressed, and the results from the current 716-level Breit–Pauli R-matrix and 262-level Dirac-R-matrix calculations showed good agreement and, for the first time, displayed near-convergence across a wide temperature range. Preliminary fine-structure resolved photoionisation cross-sections for neutral iron have been presented; however, the calculated ionisation potential was found to be larger than the measured values, which was subsequently remedied by exploring the effects of removing N+1 configurations. We have shown that removing N+1 configurations associated with some highly excited Fe II target configurations acts to correct the ionisation potential whilst preserving the magnitude and structure of the photoionisation cross-section. Results presented throughout this paper will be of use to those requiring extensive sets of accurate atomic data for Fe I and Fe II for use in the modelling of a variety of astrophysical objects.

Author Contributions: All authors contributed equally to this paper.

Conflicts of Interest: The authors declare no conflict of interest.

References

1. Eriksson, M.; Johansson, S.; Wahlgren, G.M. The nature of ultraviolet spectra of AG Pegasi and other symbiotic stars: locations, origins, and excitation mechanisms of emission lines. *Astron. Astrophys.* **2006**, *451*, 157–175. [CrossRef]
2. Smith, N.; Hartigan, P. Infrared [Fe II] Emission from P Cygni's Nebula: Atomic Data, Mass, Kinematics, and the 1600 AD Outburst. *Astrophys. J.* **2006**, *638*, 1045–1055. [CrossRef]

3.   Nussbaumer, H.; Storey, P.J. Atomic data for Fe II. *Astron. Astrophys.* **1980**, *89*, 308–313.

4.   Nussbaumer, H.; Pettini, M.; Storey, P.J. Sextet transitions in Fe II. *Astron. Astrophys.* **1981**, *102*, 351–358.

5.   Baluja, K.L.; Hibbert, A.; Mohan, M. Electron impact excitation of Fe II using the R-matrix method. *J. Phys. B At. Mol. Phys.* **1986**, *19*, 3613–3623. [CrossRef]

6.   Pradhan, A.K.; Berrington, K.A. R-matrix calculations for electron impact excitation of Fe II: LS coupling and Breit–Pauli approximations. *J. Phys. B At. Mol. Phys.* **1993**, *26*, 157–172. [CrossRef]

7.   Ramsbottom, C.A.; Scott, M.P.; Bell, K.L.; Keenan, F.P.; McLaughlin, B.M.; Sunderland, A.G.; Burke, V.M.; Noble, C.J.; Burke, P.G. Electron impact excitation of the iron peak element Fe II. *J. Phys. B At. Mol. Phys.* **2002**, *35*, 3451–3477. [CrossRef]

8.   Ramsbottom, C.A.; Noble, C.J.; Burke, V.M.; Scott, M.P.; Burke, P.G. Configuration interaction effects in low-energy electron collisions with Fe II. *J. Phys. B At. Mol. Phys.* **2004**, *37*, 3609–3631. [CrossRef]

9.   Ramsbottom, C.A.; Noble, C.J.; Burke, V.M.; Scott, M.P.; Kisielius, R.; Burke, P.G. Electron impact excitation of Fe II: Total LS effective collision strengths. *J. Phys. B At. Mol. Phys.* **2005**, *38*, 2999–3014. [CrossRef]

10.   Berrington, K.A.; Burke, P.G.; Hibbert, A.; Mohan, M.; Baluja, K.L. Electron impact excitation of Fe + using the R-matrix method incorporating fine-structure effects. *J. Phys. B At. Mol. Phys.* **1988**, *21*, 339–350. [CrossRef]

11.   Zhang, H.L.; Pradhan, A.K. Atomic data from the Iron Project. VI. Collision strengths and rate coefficients for Fe II. *Astron. Astrophys.* **1995**, *293*, 953–966.

12.   Bautista, M.A.; Pradhan, A.K. Atomic data from the Iron project. XIII. Electron excitation rates and emissivity ratios for forbidden transitions in NI II and Fe II. *Astron. Astrophys. Suppl.* **1996**, *115*, 551–559.

13.   Bautista, M.A.; Pradhan, A.K. Ionization Structure and Spectra of Iron in Gaseous Nebulae. *Astrophys. J.* **1998**, *492*, 650–676. [CrossRef]

14.   Bautista, M.A.; Fivet, V.; Ballance, C.; Quinet, P.; Ferland, G.; Mendoza, C.; Kallman, T.R. Atomic Data and Spectral Model for Fe II. *Astrophys. J.* **2015**, *808*, 174. [CrossRef]

15.   Ramsbottom, C.A.; Hudson, C.E.; Norrington, P.H.; Scott, M.P. Electron-impact excitation of Fe II*—Collision strengths and effective collision strengths for low-lying fine-structure forbidden transitions. *Astron. Astrophys.* **2007**, *475*, 765–769. [CrossRef]

16.   Ramsbottom, C. Electron-impact excitation of Fe II: Effective collision strengths for optically allowed fine-structure transitions. *At. Data Nucl. Data Tables* **2009**, *95*, 910–986. [CrossRef]

17.   Dirac R-Matrix Codes. Available online: http://connorb.freeshell.org/ (accessed on 18 June 2018).

18.   Reilman, R.F.; Manson, S.T. Photoabsorption cross sections for positive atomic ions with Z equal to or less than 30. *Astrophys. J. Suppl. Ser.* **1979**, *40*, 815–880. [CrossRef]

19.   Verner, D.; Yakovlev, D.; Band, I.; Trzhaskovskaya, M. Subshell Photoionization Cross Sections and Ionization Energies of Atoms and Ions from He to Zn. *At. Data Nucl. Data Tables* **1993**, *55*, 233–280. [CrossRef]

20.   Kelly, H.P. Photoionization Accompanied by Excitation of Fe I. *Phys. Rev. A* **1972**, *6*, 1048–1053. [CrossRef]

21.   Kelly, H.P.; Ron, A. Photoionization Cross Section of the Neutral Iron Atom. *Phys. Rev. A* **1972**, *5*, 168–176. [CrossRef]

22.   Sawey, P.M.J.; Berrington, K.A. Atomic data for opacity calculations. XV. Fe I-IV. *J. Phys. B At. Mol. Phys.* **1992**, *25*, 1451–1466. [CrossRef]

23.   Bautista, M.A. Atomic data from the IRON Project—XX. Photoionization cross sections and oscillator strengths for Fe I. *Astron. Astrophys. Suppl. Ser.* **1997**, *122*, 167–176. [CrossRef]

24.   Bautista, M.A.; Pradhan, A.K. Photoionization of neutral iron. *J. Phys. B At. Mol. Phys.* **1995**, *28*, L173–L179. [CrossRef]

25.   Sawey, P.M.J.; Berrington, K.A. Resonances due to photoexcitation of the core in the photoionization cross section for excited states of iron. *J. Phys. B At. Mol. Phys.* **1990**, *23*, L817–L822. [CrossRef]

26.   Bautista, M.A.; Lind, K.; Bergemann, M. Photoionization and electron impact excitation cross sections for Fe. *Astron. Astrophys.* **2017**, *606*, A127. [CrossRef]

27.   Berrington, K.A.; Ballance, C. Double ionization yields from the photoionization of Fe II and Fe I. *J. Phys. B At. Mol. Phys.* **2001**, *34*, L383. [CrossRef]

28.   Baluja, K.L.; Butler, K.; Le Bourlot, J.; Zeippen, C.J. Recent radiative and collisional atomic data of astrophysical interest. *J. Phys. Colloques* **1988**, *49*, C1-129–C1-132. [CrossRef]

29.   Fivet, V.; Bautista, M.A.; Ballance, C.P. Fine-structure photoionization cross sections of Fe II. *J. Phys. B At. Mol. Phys.* **2012**, *45*, 035201. [CrossRef]

30. Nahar, S.N. Relativistic photoionization cross sections for C II. *Phys. Rev. A* **2002**, *65*, 052702. [CrossRef]
31. Hibbert, A. CIV3—A general program to calculate configuration interaction wave functions and electric-dipole oscillator strengths. *Comput. Phys. Commun.* **1975**, *9*, 141–172. [CrossRef]
32. Dyall, K.; Grant, I.; Johnson, C.; Parpia, F.; Plummer, E. GRASP: A general-purpose relativistic atomic structure program. *Comput. Phys. Commun.* **1989**, *55*, 425–456. [CrossRef]
33. Parpia, F.A.; Grant, I.P. Software for relativistic atomic theory: The GRASP project at Oxford. *J. Phys. IV Fr.* **1991**, *1*, C1-33–C1-46. [CrossRef]
34. NIST. Available online: http://www.nist.gov/pml/data/asd.cfm (accessed on 18 June 2018).
35. Keenan, F.P.; Hibbert, A.; Burke, P.G.; Berrington, K.A. Fine-structure populations for the 6D ground state of Fe II. *Astrophys. J.* **1988**, *332*, 539–542. [CrossRef]